ISSN 1392–1320 MATERIALS SCIENCE (MEDŽIAGOTYRA). Vol. 20, No. 1. 2014

Sol-gel Derived Europium Doped $CaMoO_4:Eu^{3+}$ with Complex Microstructural and Optical Properties

Gediminas BRAZIULIS, Ruta STANKEVICIUTE, Arturas ZALGA *

Department of Inorganic Chemistry, Vilnius University, Naugarduko 24, LT-03225 Vilnius, Lithuania

crossref http://dx.doi.org/10.5755/j01.ms.20.1.4797

Received 16 July 2013; accepted 13 October 2013

The crystalline compounds $CaMoO_4$ doped with Eu^{3+} ions were prepared from nitrate-tartrate precursor gels at 650, 700, 750 and 800 °C temperatures. The obtained samples were characterized by thermal analysis (TG/DSC), Furier Transform infrared spectroscopy (FT-IR), X-ray diffraction (XRD) analysis, scanning electron microscopy (SEM) and reflection measurements (UV-vis). TG/DSC analysis revealed the possible decomposition mechanism of synthesized Ca-Mo-O nitrate-tartrate gel. XRD data exhibited that even at 650 °C temperature the crystalline powelite ($CaMoO_4$) structure has formed. To understand the crystal growth process of the $CaMoO_4:xEu^{3+}$ compounds (x = 1, 2, 3, 4, 5 and 6 mol%), the influence of temperature on the surface morphology of the end products by SEM analysis was investigated. No evidence of organic residual in the final materials was found, confirmed by FT-IR analysis. UV-vis reflectance spectra revealed that by increasing of Eu^{3+} ions concentrations in the host material the reflection peaks of Eu_2O_3 also increased.
Keywords: inorganic compounds, optical materials, sol-gel synthesis, microstructure.

1. INTRODUCTION

In recent years, the optical properties of trivalent rare-earth ions (RE^{3+}) in tungstate and molybdate materials with scheelite ($CaWO_4$) and isostructural powelite ($CaMoO_4$) structures have been widely investigated [1]. Especially, many researchers focused their attention on europium (III) ions as luminescence centres in red light phosphors with excellent luminescent properties [2]. It is well known that rare-earth elements have been widely used in high-performance luminescence devices, catalysts and other functional materials because of the electronic, optical and chemical characteristics originating from their 4f electrons [3]. The red luminescence of Eu^{3+} ion has been extensively used in the lighting and displays for its distinct 4f-4f transitions. The f-electron of Eu^{3+} ions are well shielded from the chemical environment and own almost retained atomic character [4].

Metal molybdates are important family of inorganic materials that have great potential applications in various fields, such as phosphors [5], optical fibers [6], scintillators [7], magnets [8] and catalysts [9]. As was mentioned above, calcium molybdate ($CaMoO_4$) crystal possesses the powelite structure (tetragonal, space group I41/a) [10], and has been attracting much attention because of its high applications as a potential acousto-optic filtration [11], electron conduction [12], or photoluminescence emission (PL) [13].

Several methods have been developed to prepare $CaMoO_4$ such as traditional solid-state reaction [14], the coprecipitation [15] synthesis, the combustion method [16], Czochralski method [17], solvothermal process [18], reverse micellar reaction [19], microwave irradiation [20], spray pyrolysis [21], the facile microemulsion-mediated hydrothermal process [22], electrochemical method [23], sonochemical preparation [24] and sol-gel synthesis [25]. Among these different synthesis routes the solution based synthetic methods play a crucial role in the design and production of fine ceramics and have been successful in overcoming many of the limitation of the traditional solid-state, high-temperature methods. The use of solution chemistry can eliminate major problems such as long diffusion paths, impurities and agglomeration, which will result in products with improved homogeneity [26]. The metal complexes with organic ligands have been used for the preparation of ceramics and metal oxides thin films by sol-gel process, using metal salts like nitrates [27], chlorides [28], and acetates [29] as starting materials. In this paper we report the synthesis of powellite type $CaMoO_4$ doped with Eu^{3+} ions by a novel aqueous sol-gel synthesis route. In the sol-gel process tartaric acid as a complexing agent has been used.

2. EXPERIMENTAL DETAILS

2.1. Sample preparation

The samples $CaMoO_4:Eu^{3+}$ with 1, 2, 3, 4, 5 and 6 mol% of Eu^{3+} were prepared by an aqueous nitrate-tartrate sol-gel route. The europium oxide (Eu_2O_3, 99.99 %), molybdenum oxide (MoO_3, 99.95 %), calcium nitrate tetrahydrate ($Ca(NO_3)_2 \cdot 4H_2O$, 99 %) were used as starting materials and weighed according to the desired stoichiometric ratio. Nitric acid (HNO_3) and ammonia ($NH_3 \cdot 4H_2O$) were used as solvents and reagents to regulate the pH of the solutions. Tartaric acid (TA, $C_4H_6O_6$, 99.5 %) was used as a complexing agent. In the sol-gel process, MoO_3 was dissolved in 25 mL of concentrated ammonia solution by stirring at 70 °C – 80 °C. Secondly, tartaric acid with a molar ratio of Mo / TA = 0.25, dissolved in a small amount of distilled water was added with a continuous stirring at the same temperature. Next, after several hours the stoichiometric amount of calcium

*Corresponding author. Tel.: +370-5-2193107, fax: +370-5-2330987.
E-mail address: *arturas.zalga@chf.vu.lt* (A. Zalga)

nitrate tetrahydrate dissolved in distilled water was mixed with the previous solution. To prevent precipitation, the excess of ammonia was neutralized with concentrated HNO_3 until the pH reached the value of ~1.0. Afterwards, Eu_2O_3 was added directly to the reaction mixture. Finally, the same amount of the aqueous solution of the complexing agent TA was repeatedly added to the reaction mixture to prevent crystallization of metal salts during the gelation process. The beaker with the solution was closed with a watch glass and left for 1 h with continuous stirring. The obtained clear solution was concentrated by slow evaporation at 80 °C in an open beaker. A yellow transparent gel formed after nearly 95 % of the water has been evaporated under continuous stirring. After drying in an oven at 110 °C, fine-grained powders were obtained. The precursor gels were calcined for 5 h at 500 °C in alumina crucibles and reground carefully in an agate mortar. The five hours of the annealing temperature was chosen because of the full combustion of organic parts in the sample. Since the gels are very combustible, slow heating (1 °C/min), especially between 150 °C and 300 °C, was found to be essential. After intermediate grinding the obtained powders for 5 h at 650, 700, 750 and 800 °C temperatures in air at ambient pressure were annealed.

2.2. Characterization

The thermal decomposition of complex precursor gel was examined by thermogravimetry-differential scanning calorimetry (TG-DSC, Netzsch STA 449C Jupiter instrument) using a sample weight of about 10 mg and a heating rate of 5 °C·min^{-1} in flowing air (70 cm^3·min^{-1}) at ambient pressure from room temperature to 1000 °C. The synthesized samples were characterized by X-ray powder analysis (D8 Bruker AXS powder diffractometer) using $CuK_{\alpha 1}$ radiation. The spectra were recorded at the standard rate of 1.5 2θ/min. After pressing the samples into the pellets with KBr (~1.5 %), the Fourier transform infrared (FT-IR) spectra were recorded with a Perkin-Elmer FT-IR Spectrum 1000 spectrometer. The scanning electron microscope (SEM) DSN 962 was used to study the surface morphology and microstructure of the obtained ceramic samples. The reflection spectra were recorded at room temperature using a Perkin Elmer Lambda 35 UV/VIS spectrometer. The samples were well glued up on the flat substrate in order to form thin layer on it and excited in 1100 nm – 200 nm wavelength interval.

3. RESULTS AND DISCUSSION

3.1. Thermal analysis

The TG-DSC curves of the $CaMoO_4$ precursor gel displayed in Fig. 1. These results let us understand its pyrolysis behaviour and crystallization process. The TG curve indicates that by increasing the temperature from up to 530 °C the weight loss of the Ca-Mo-O nitrate-tartrate precursor gel occurs. The decomposition process can be roughly divided into three intervals. The first weight loss observed between room temperature and 180 °C in the TG curve could be attributed to the removal water from the coordination sphere of the metal complexes and/or of surface adsorbed water. A strong endothermic peak near 175 °C in the DSC curve confirms the dehydratation process in this temperature region. With further increasing temperature from 200 °C up to 450 °C the second main weight loss occurred which is attributed to the pyrolysis of the organic part of the gel and the decomposition of corresponding metal nitrates, as indicated by weight loss about 60 % on the TG curve.

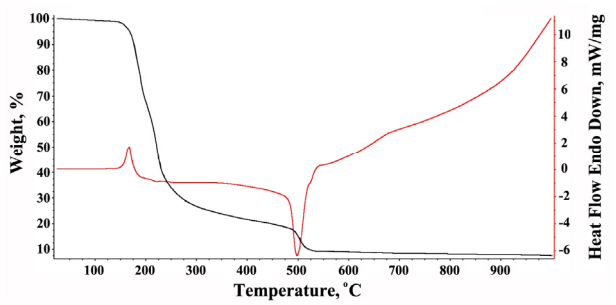

Fig. 1. Combined TG-DSC curves of the $CaMoO_4$ precursor gel in flowing air

Thereafter, the weight loss of about 10 % observed in the temperature range from 480 °C to 520 °C is associated with further decomposition of the intermediate pyrolysis products (carbonates or oxycarbonates). Finally, the weight remains almost constant up to 1000 °C, which indicates that the decomposition and combustion of all organic components in the precursor gel is completed below 530 °C. The sharp exothermic peak at about 500 °C on the DSC curve could be attributed to the final burning of the residual organic species in the Ca-Mo-O gel. The negligible peaks on the DSC curve at ~530 °C and ~670 °C correspond probably to the crystallization of $CaMoO_4$. Therefore, we can conclude from Fig. 1, that crystalline $CaMoO_4$ homogeneously doped with Eu_2O_3 could be obtained at around 650 °C, which was proved by XRD measurements.

3.2. X-ray diffraction

Fig. 2 exhibits the X-ray diffraction (XRD) patterns of the $CaMoO_4$: 1 % Eu^{3+} powders obtained by sintering the dried gels for 5 h at 650, 700, 750 and 800 °C temperatures. As seen, the calcination of Ca(Eu)-Mo-O nitrate-tartrate precursor gel powders at different temperatures produces a fully crystalline $CaMoO_4$ phase and no characteristic peaks due to the side crystalline Eu_2O_3 or Eu_2MoO_6 phases were observed. When the dried gels were calcined at 650, 700, 750 and 800 °C temperatures only the tetragonal $CaMoO_4$ phase appeared, which corresponds to ICSD file number 62219. These results clearly indicate that the crystallization of the $CaMoO_4$ phase is entirely complete at the relatively low temperature of 650 °C and this is in a good agreement with the TG-DSC results. However, some low intense impurity peaks in the XRD pattern of the powders calcined at 700 °C (see Figs. 2 and 3) could be indexed as a MoO_3 crystalline phase. In addition, no characteristic peaks attributable to the CaO crystal phase were indentified. On the other hand, by further increasing sintering time and temperature the diffraction lines from impurity phase disappeared, and the XRD patterns of the samples annealed at 750 °C and 800 °C temperatures showed only monophasic crystalline $CaMoO_4$ (Fig. 2).

It is interesting to note, that this aqueous sol-gel synthesis route from metal nitrate precursors in the sol-gel process using tartaric acid, as a complexing agent could be successful used for the preparation of thin film on glass or silicon substrates. The obtained specimens now are under investigation.

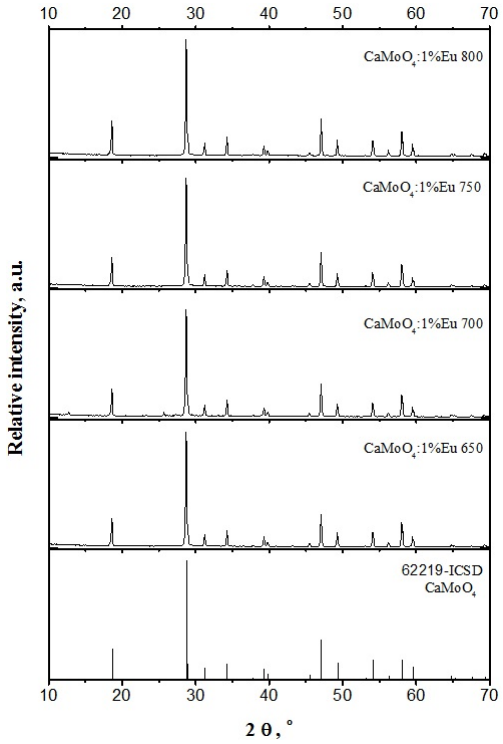

Fig. 2. XRD patterns of the $CaMoO_4 : 1\ \% Eu^{3+}$ precursors heat-treated at 650, 700, 750, 800 °C, and standard ICSD card of tetragonal $CaMoO_4$ (62219)

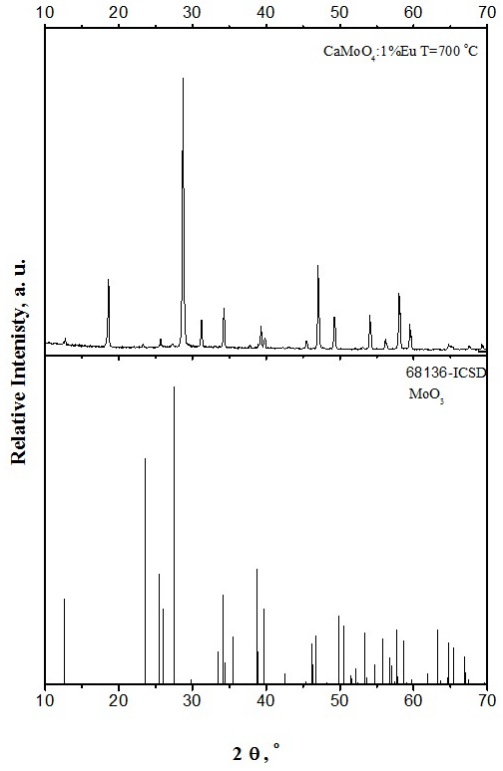

Fig. 3. XRD pattern of the $CaMoO_4 : 1\ \% Eu^{3+}$ precursors heat-treated at 700 °C and standard ICSD card of MoO_3 (68136)

3.3. FT-IR analysis

The infrared spectra of the synthesized $CaMoO_4$:xEu^{3+} samples annealed at 650 °C for 5 h are shown in Fig. 4. All FT-IR spectra of the $CaMoO_4 : x\ Eu^{3+}$ specimens qualitatively are very similar regardless the concentration of europium in the material. Interestingly, the FT-IR spectra of $CaMoO_4 : x\ Eu^{3+}$ compounds have approximately the same vibration modes as the $CaWO_4 : Eu^{3+}$ phosphor [30].

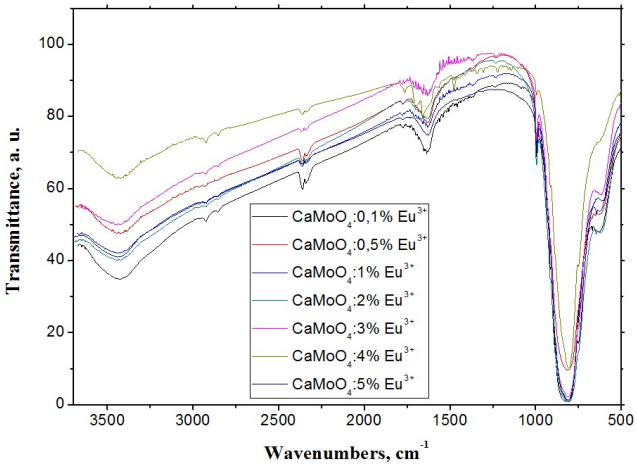

Fig. 4. FT-IR absorption spectra of $CaMoO_4 : x\ Eu^{3+}$ samples

The bands at 3454 cm^{-1} and 1631 cm^{-1} are assigned to O–H stretching vibration and H–O–H bending vibrations [31], respectively. These two bands are the characteristic vibrations of water from air, physically absorbed on the sample surface that is completely different from coordinated water in compound. A strong absorption band at around 910 cm^{-1} is related to O–Mo–O stretches of the MoO_4 tetrahedron. The AWO_4 type scheelite oxides having S_4 symmetry for the WO_4^{2-} groups also show the main absorption bands in the region of 400 cm^{-1} – 1000 cm^{-1}, centered around 911, 833 and 405 cm^{-1} corresponding to the ν1, ν3 and ν2 modes of the WO_4^{2-} groups, respectively [1]. It is also important to note, that the FT-IR spectra of Eu_2O_3 doped calcium molybdate samples calcined at 650 °C did not show any bands attributable to carbonates or residual organic species.

3.4. SEM microscopy

To understand the crystal growth process of the $CaMoO_4 : x\ Eu^{3+}$ compounds, we investigated the influence of temperature on the morphology of the products. The SEM micrographs of $CaMoO_4 : x\ Eu^{3+}$ samples prepared by the an aqueous sol-gel method at 650, 700, 750 and 800 °C are shown in Figs. 5 – 10. The SEM results clearly indicate that all products consist of micrometer and sub-micrometer differently shaped particles with narrow crystal size distribution. The homogeneous spherical grains of $CaMoO_4 : 1\ \% Eu^{3+}$ with an average diameter of about 1 μm – 5 μm have formed when the synthesis was carried out at 650 °C (Fig. 5).

As seen from micrographs at higher magnification (Fig. 5, c and d), the surface morphology of synthesized samples exhibits homogeneous packing of the micrograins where the larger particles (about 5 μm) are surrounded

with smaller grains of about 1 μm diameter. However, the SEM image of $CaMoO_4:6\ \%\ Eu^{3+}$ compound (Fig. 6, a) reveals the formation of plate-like larger crystals in size of about 15 μm – 20 μm.

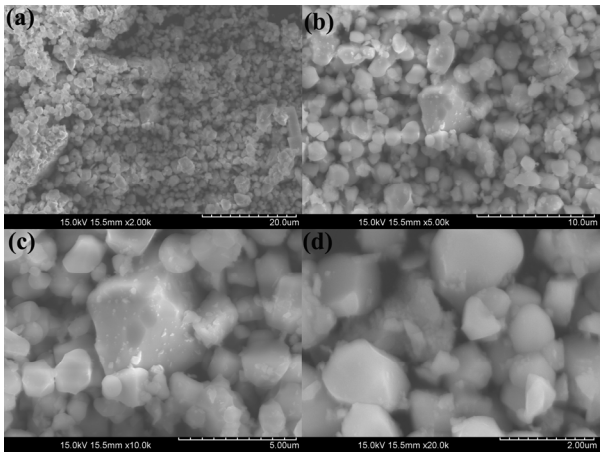

Fig. 5. SEM micrographs of 1 % Eu^{3+} ions doped $CaMoO_4$ sample synthesized at 650 °C in air atmosphere

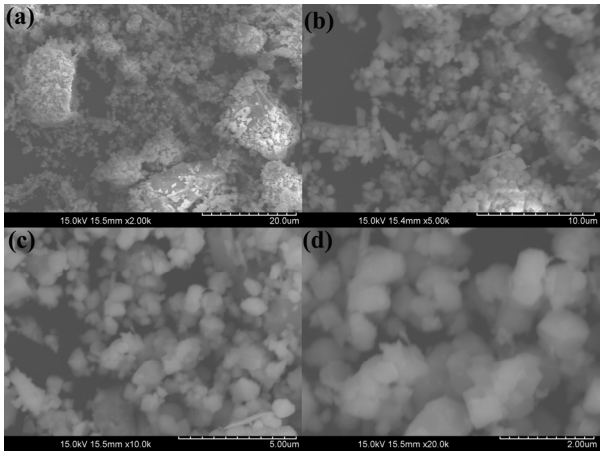

Fig. 6. SEM micrographs of 6 % Eu^{3+} ions doped $CaMoO_4$ sample synthesized at 650 °C air atmosphere

These crystallites co-exist in close packing with spherical particles of size less than 2 μm (Fig, 6, b, c and d), indicating that the concentration of dopant has a small effect on the morphological features of the molybdate samples annealed at the 650 °C.

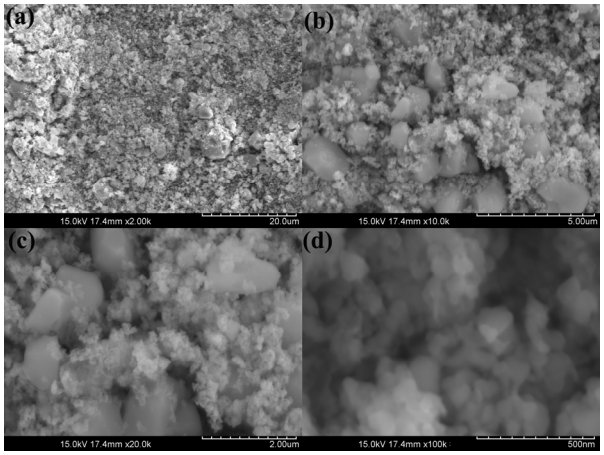

Fig. 7. SEM micrographs of 1 % Eu^{3+} ions doped $CaMoO_4$ sample synthesized at 700 °C in air atmosphere

As shown in Fig. 7, a – d, with increasing sintering temperature up to 700 °C two types of grains have formed. The smaller spherical particles, which are less than 200 nm size, tend to aggregate by many small crystal grains. Meanwhile, the larger grains form individual crystals rather than aggregate with each other. This observation could explain the impurity phase of MoO_3 in XRD pattern of the $CaMoO_4:1\ \%\ Eu^{3+}$ sample prepared at 700 °C for 5 h in air atmosphere.

With further increasing the temperature up to 750 °C, the particles tend to aggregate strongly showing good connectivity between grains (Fig. 8).

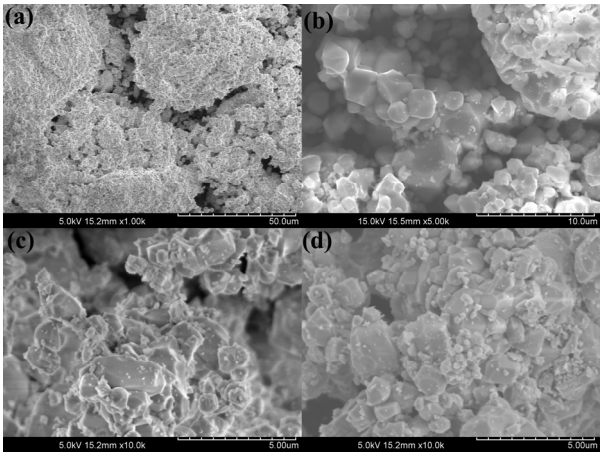

Fig. 8. SEM micrographs of 1% Eu^{3+} ions doped $CaMoO_4$ sample synthesized at 750 °C in air atmosphere

Less than 3 μm plate-like crystals with narrow size distribution $CaMoO_4:1\ \%\ Eu^{3+}$ sample have formed at this temperature. Fig. 9 shows the SEM micrograph of the $CaMoO_4:1\ \%\ Eu^{3+}$ sample synthesized at 800 °C for 5 h in air atmosphere.

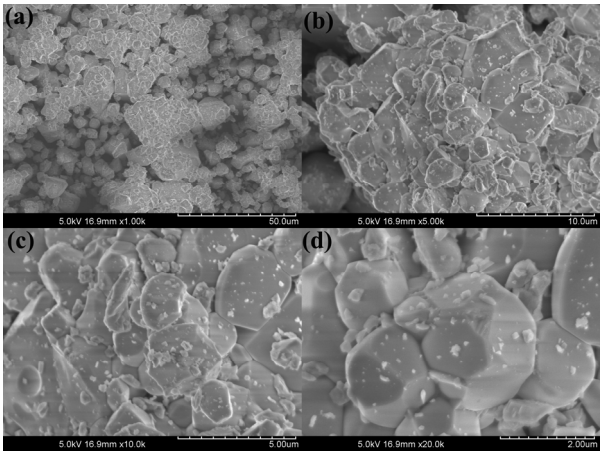

Fig. 9. SEM micrographs of 1% Eu^{3+} ions doped $CaMoO_4$ sample synthesized at 800 °C in air atmosphere

However, the surface morphology of the $CaMoO_4:1\ \%\ Eu^{3+}$ powders synthesized at 800 °C for 5h are very similar to those prepared at 750 °C. The higher temperature produced just a bit larger crystals. Fig. 10 represents the SEM image of $CaMoO_4:6\ \%\ Eu^{3+}$ synthesized at 800 °C for 5 h in air atmosphere. Again, with increasing concentration of europium the larger crystallites of the ceramic material have formed.

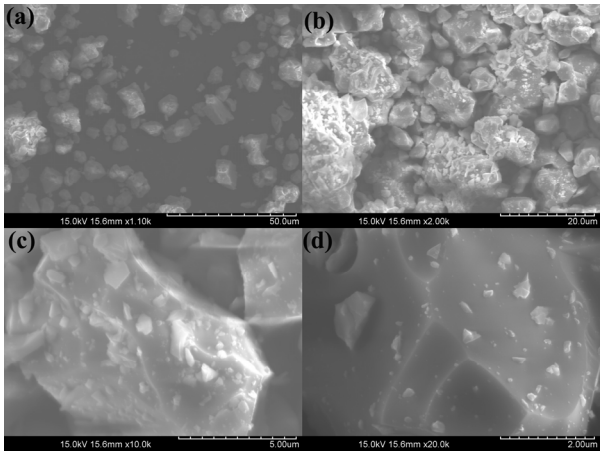

Fig. 10. SEM micrographs of 6 % Eu^{3+} ions doped $CaMoO_4$ sample synthesized at 800 °C in air atmosphere

The high-magnification SEM images (Fig. 10, c and d) revealed that synthesized products consist of different crystallites with diameter of 2 μm – 4 μm and length 5 μm – 7 μm. These SEM results of the $CaMoO_4 : x\ \%\ Eu^{3+}$ samples annealed at different temperatures confirmed that the sintering temperature and the dopant concentration could strongly affect on the morphological features of final products.

3.5. Reflection measurements

The optical properties of doped with europium $CaMoO_4$ ceramics synthesized using the nitrate-tartrate sol-gel technique were also investigated. UV-vis reflectance spectra of $CaMoO_4 : x\ \%\ Eu^{3+}$ (x = 1, 2, 3, 4, 5 and 6) phosphor are shown in Figs. 11 – 13.

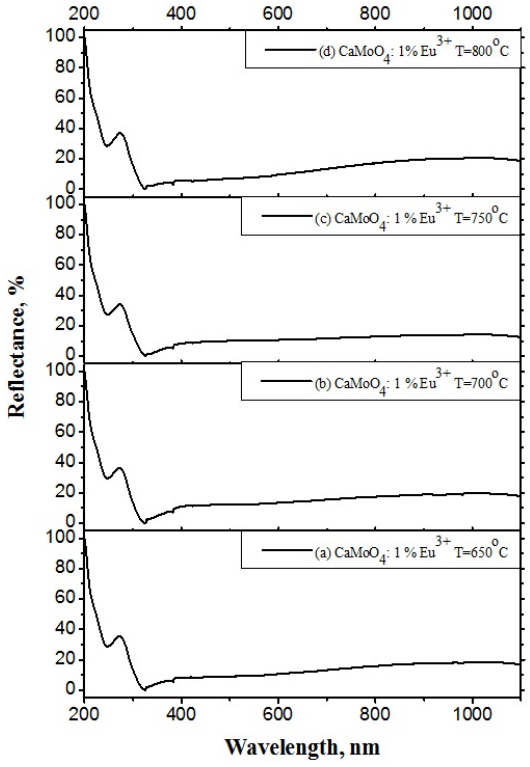

Fig. 11. UV-vis reflectance spectra of crystalline $CaMoO_4$ doped with 1 % Eu^{3+} ions and annealed at 650 °C (a), 700 °C (b), 750 °C (c) and 800 °C (d) temperatures

According to the results presented in [33], $CaMoO_4$ nano-crystals exhibited a very broad asymmetric reflection in the range of 180 nm – 300 nm, which is also observed in Fig. 11 of the $CaMoO_4 : 1\ \%\ Eu^{3+}$ samples annealed at 650 °C – 800 °C temperatures. Additionally, the reflectance spectra of all samples are very similar. The reflection bands of $CaMoO_4 : 1\ \%\ Eu^{3+}$ samples are located between 200 nm and 315 nm, corresponding to oxygen to molybdenum (O→Mo) ligand-to-metal charge transfer in the MoO_4^{2-} group. As is shown in Fig. 12, the reflection bands at 362, 367, 377, 382, 385 nm and sharp peaks at 394, 465 nm could be attributed to the reflectance of Eu^{3+} ions in the $CaMoO_4$ host-lattice. Moreover, the sharp peak at 394.8 nm tends to increase (see Fig. 13) by increasing dopant concentration in $CaMoO_4$ host-lattice. However, the peak intensity of the $CaMoO_4 : x\ \%\ Eu^{3+}$ samples annealed at 750 °C reached the maximum only with doping of 5 mol% of Eu^{3+} ions and further increasing of dopant concentration leads to the quenching of reflectance of obtained optical materials.

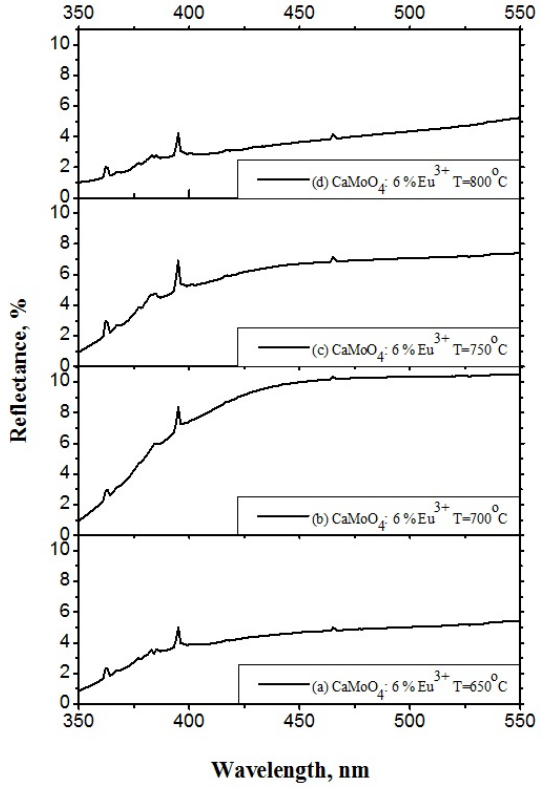

Fig. 12. UV-vis reflectance spectra of crystalline $CaMoO_4$ doped with 6 % Eu^{3+} ions and annealed at 650 °C (a), 700 °C (b), 750 °C (c) and 800 °C (d) temperatures

As can be seen from Fig. 12, the annealing temperature only little affects the optical properties of $CaMoO_4$ doped with 6 % of Eu^{3+}. The maximum intensity of reflection peak at 394.8 nm of excitation light achieved in the sample synthesized at 750 °C temperature.

In conclusion, it should be noted that all synthesized $CaMoO_4 : x\ Eu^{3+}$ samples were optically active compounds at shorter wavelengths (200 nm – 310 nm) that arises from MoO_4^{2-}. Reflection peaks in 360 nm–470 nm wavelength region are attributed to the Eu^{3+} characteristic excitations, which are significantly influenced both by annealing temperature and by dopant concentration in $CaMoO_4$ lattice.

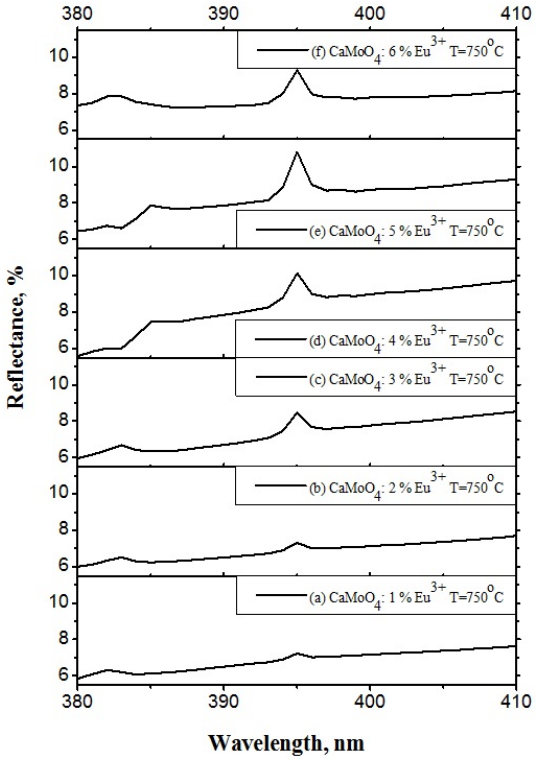

Fig. 13. UV-vis reflectance spectra of $CaMoO_4 : 1\ \% Eu^{3+}$ (a), $CaMoO_4 : 2\ \% Eu^{3+}$ (b), $CaMoO_4 : 3\ \% Eu^{3+}$ (c), $CaMoO_4 : 4\ \% Eu^{3+}$ (d) $CaMoO_4 : 5\ \% Eu^{3+}$ (e), $CaMoO_4 : 6\ \% Eu^{3+}$ (f) annealed at 750 °C

4. CONCLUSIONS

Single-phase $CaMoO_4 : x\ Eu^{3+}$ (x = 1, 2, 3, 4, 5 and 6 mol% Eu^{3+}) phosphors with 1 μm – 7 μm dimensions were prepared by an aqueous nitrate-tartrate sol-gel processing. According to the XRD data, the crystallization of the $CaMoO_4$ precursors is entirely complete at relatively low temperature of 650 °C and is in consonant with the results of TG-DSC. However, by increasing sintering temperature up to 700 °C the small amount of MoO_3 impurity phase have formed. With further increasing temperature (750 °C and 800 °C) the XRD patterns of europium doped $CaMoO_4$ showed the formation of only pure crystalline molybdate phase. It was demonstrated, that the morphology and crystallite size of $CaMoO_4 : Eu^{3+}$ samples are dependent on the annealing temperature and dopant concentration. Moreover, the reflection measurements of the synthesized $CaMoO_4 : Eu^{3+}$ samples clearly showed that all synthesized $CaMoO_4 : xEu^{3+}$ specimens are optical active compounds.

Acknowledgments

The study was funded from the European Community's social foundation under Grant Agreement No. VP1-3.1-ŠMM-08-K-01-004/KS-120000-1756.

REFERENCES

1. **Lei, F., Yan, B.** Hydrothermal Synthesis and Luminescence of $CaMO_4 : RE^{3+}$ (M = W, Mo; RE = Eu, Tb) Submicrophosphors *Journal of Solid State Chemistry* 181 2008: pp. 855 – 862. http://dx.doi.org/10.1016/j.jssc.2008.01.033
2. **Wei, Q., Chen, D. H.** Luminescence Properties of Eu^{3+} and Sm^{3+} Coactivated Gd(III) Tungstate Phosphor for Light-emitting Diodes *Optics and Laser Technology* 41 2009: pp. 783 – 787. http://dx.doi.org/10.1016/j.optlastec.2008.12.003
3. **Fu, L., Liu, Z. M., Liu, Y. Q., Han, B. X., Wang, J. Q., Hu, P. G., Cao, L. C., Zhu, D. B.** Coating Carbon Nanotubes with Rare Earth Oxide Multiwalled Nanotubes *Advanced Materials* 16 2004: pp. 350 – 352.
4. **Tang, Z., Zhou, L., Wang, F., Zhou, L.** Synthesis, Characterization and Luminescence Study of Eu(III) Tungstates and Molybdates Nanotubes Using Carbon Nanotubes as Templates *Spectrochimica Acta Part A Molecular and Biomolecular Spectroscopy* 72 2009: pp. 348 – 355. http://dx.doi.org/10.1016/j.saa.2008.10.010
5. **Guo, C. F., Zhang, W., Luan, L., Chen, T., Cheng, H., Huang, D. X.** A Promising Red-emitting Phosphor for White Light Emitting Diodes Prepared by Sol-gel Method *Sensors and Actuators B-Chemical* 133 2008: pp. 33 – 39.
6. **Tanaka, K., Miyajima, T., Shirai, N., Zhuang, Q., Nakata, R.** Laser Photochemical Ablation of $CdWO_4$ Studied with the Time-of-Flight Mass-Spectrometric Technique *Journal of Applied Physics* 77 1995: pp. 6581 – 6587. http://dx.doi.org/10.1063/1.359067
7. **Kwan, S., Kim, F., Akana, J., Yang, P. D.** Synthesis and Assembly of $BaWO_4$ Nanorods *Chemical Communications* 5 2001: pp. 447 – 448. http://dx.doi.org/10.1039/b100005p
8. **Isayama, A., Kadota, S., Yui, H., Sasagawa, T.** Chemical Pressure Effects on Magnetic Properties of A_2FeMoO_6 (A = Ca, Sr, and Ba) *Materials Science and Engineering B Advanced Functional Solid-State Materials* 173 2010: pp. 44 – 46.
9. **Malka, K., Tatibouet, J. M.** A Two-step Preparation of Silica-supported Calcium-molybdenum Catalysts *Journal of Catalysis* 175 1998: pp. 204 – 212.
10. **Zhang, Y., Holzwarth, N. A. W., Williams, R. T.** Electronic Band Structures of the Scheelite Materials $CaMoO_4$, $CaWO_4$, $PbMoO_4$, and $PbWO_4$ *Physical Review B* 57 1998: pp. 12738 – 12750. http://dx.doi.org/10.1103/PhysRevB.57.12738
11. **Mazur, M. M., Makhmudov, K. M., Pustovolt, V. J.** Tunable Dye Laser with an Acoustooptic $CaMoO_4$ Filter *Soviet Journal of Quantum Electronics* 18 1988: p. 453. doi:10.1070/QE1988v018n04ABEH011551.
12. **Petrov, A., Kofstad, P.** Electrical Conductivity of $CaMoO_4$ *Journal of Solid State Chemistry* 30 (1) 1979: pp. 83 – 88. http://dx.doi.org/10.1016/0022-4596(79)90133-6
13. **Grasser, R., Pitt, E., Scharmann, A., Zimmerer, G.** Optical Properties of $CaWO_4$ and $CaMoO_4$ Crystals in the 4 to 25 eV Region *Physica Status Solidi B* 69 (2) 1975: pp. 359 – 368. http://dx.doi.org/10.1002/pssb.2220690206
14. **Marques, A. P. D., Longo, V. M., de Melo, D. M. A., Pizani, P. S., Leite,E. R., Varela, J. A., Longo, E.** Shape Controlled Synthesis of $CaMoO_4$ Thin Films and Their Photoluminescence Property *Journal of Solid State Chemistry* 181 2008: pp. 1249 – 1257.
15. **Bosbach, D., Rabung, T., Luckscheiter, B.** Cm^{3+}/Eu^{3+} Coprecipitation with Powellite ($CaMoO_4$) During HLW Glass Corrosion *Geochimica Et Cosmochimica Acta* 66 2002: pp. A93 – A93.

16. **Yang, P., Yao, G. Q., Lin, J. H.** Photoluminescence and Combustion Synthesis of $CaMoO_4$ Doped with Pb^{2+}, *Inorganic Chemistry Communications* 7 2004: pp. 389 – 391. http://dx.doi.org/10.1016/j.inoche.2003.12.021
17. **Jia, G. H., Tu, C. Y., You, Z. Y., Li, J. F., Zhu, Z. J., Wang, Y., Wu, B. C.** Czochralski Technique Growth of Pure and Rare-earth-doped $SrWO_4$ Crystals *Journal of Crystal Growth* 273 2004: pp. 220 – 225. http://dx.doi.org/10.1016/j.jcrysgro.2004.07.095
18. **Byun, H. J., Song, W. S., Kim, Y. S., Yang, H.** Solvothermally Grown Ce^{3+}-doped $Y_3Al_5O_{12}$ Colloidal Nanocrystals: Spectral Variations and White LED Characteristics *Journal of Physics D Applied Physics* 43 (19) 2010. doi 10.1088/0022-3727/43/19/195401.
19. **Hirai, T., Asada, Y., Komasawa, I.** Preparation of $Y_2O_3 : Eu^{3+}$ Nanoparticles in Reverse Micellar Systems and Their Photoluminescence Properties *Journal of Colloid and Interface Science* 276 2004: pp. 339 – 345.
20. **Thongtem, T., Kaowphong, S., Thongtem, S.** Influence of Cetyltrimethylammonium Bromide on the Morphology of AWO_4 (A = Ca, Sr) Prepared by Cyclic Microwave Irradiation *Applied Surface Science* 254 2008: pp. 7765 – 7769.
21. **Sivakumar, R., Raj, A. M. E., Subramanian, B., Jayachandran, M., Trivedi, D. C., Sanjeeviraja, C.** Preparation and Characterization of Spray Deposited N-type WO_3 Thin Films for Electrochromic Devices *Materials Research Bulletin* 39 2004: pp. 1479 – 1489.
22. **Gong, Q., Li, G., Qian, X. F., Cao, H. L., Du, W. M., Ma, X. D.** Synthesis of Single Crystal $CdMoO_4$ Octahedral Microparticles via Microemulsion-mediated Route *Journal of Colloid and Interface Science* 304 2006: pp. 408 – 412. http://dx.doi.org/10.1016/j.jcis.2006.09.050
23. **Sun, Y., Ma, J. F., Jiang, X. H., Fang, J. R., Song, Z. W., Gao, C., Liu, Z. S.** Ethylene Glycol-assisted Electrochemical Synthesis of $CaMoO_4$ Crystallites with Different Morphology and Their Luminescent Properties *Solid State Sciences* 12 2010: pp. 1283 – 1286.
24. **Phuruangrat, A., Thongtem, T., Thongtem, S.** Analysis of Lead Molybdate and Lead Tungstate Synthesized by a Sonochemical Method *Current Applied Physics* 10 2010: pp. 342 – 345.
25. **Zalga, A., Juskenas, R., Selskis, A., Jasaitis, D., Kareiva, A.** Synthesis and Characterization of Ln-123 Superconductors *Journal of the Serbian Chemical Society* 73 2008: pp. 479 – 486. http://dx.doi.org/10.2298/JSC0804479Z
26. **Parhi, P., Karthik, T. N., Manivannan, V.** Synthesis and Characterization of Metal Tungstates by Novel Solid-state Metathetic Approach *Journal of Alloys and Compounds* 465 2008: pp. 380 – 386.
27. **Zalga, A., Beganskiene, A., Kareiva, A.** Sol-gel Synthesis and Superconducting Properties of Bi-2212 High-T-C Superconductors *Polish Journal of Chemistry* 81 2007: pp. 1547 – 1553.
28. **Zalga, A., Reklaitis, J., Norkus, E., Beganskiene, A., Kareiva, A.** A Comparative Study of $YBa_2Cu_4O_8$ (Y-124) Superconductors Prepared by a Sol-gel Method *Chemical Physics* 327 2006: pp. 220 – 228.
29. **Kodaira, C. A., Brito, H. F., Felinto, M. C. F. C.** Luminescence Investigation of Eu^{3+} Ion in the $RE_2(WO_4)_3$ Matrix (RE = La and Gd) Produced Using the Pechini Method *Journal of Solid State Chemistry* 171 2003: pp. 401 – 407. http://dx.doi.org/10.1016/S0022-4596(02)00221-9
30. **Zalga, A., Sazinas, R., Garskaite, E., Kareiva, A., Bareika, T., Tamulaitis, G., Juskenas, R., Ramanauskas, R.** Sol-gel Synthesis of RE^{3+}-activated $CaWO_4$ Phosphores *Chemija* 20 2009: pp. 169 – 174.
31. **Kato, A., Oishi, S., Shishido, T., Yamazaki, M., Iida, S.** Evaluation of Stoichiometric Rare-earth Molybdate and Tungstate Compounds as Laser Materials *Journal of Physics and Chemistry of Solids* 66 2005: pp. 2079 – 2081.
32. **Su, Y. G., Li, G. S., Xue, Y. F., Li, L. P.** Tunable Physical Properties of $CaWO_4$ Nanocrystals via Particle Size Control *Journal of Physical Chemistry C* 111 2007: pp. 6684 – 6689. http://dx.doi.org/10.1021/jp068480p